Coupling of Biokinetic and Population Balance Models to Account for Biological Heterogeneity in Bioreactors

Jérôme Morchain, Jean-Christophe Gabelle, and Arnaud Cockx
INSA, UPS, INP, LISBP, Université de Toulouse, 135 Avenue de Rangueil, F-31077 Toulouse, France

INRA, UMR792 Ingénierie des Systèmes Biologiques et des Procédés, F-31400 Toulouse, France

CNRS, UMR5504, F-31400 Toulouse, France

DOI 10.1002/aic.13820
Published online May 3, 2012 in Wiley Online Library (wileyonlinelibrary.com).

The development of a population balance model accounting for cell adaptation to a fluctuating environment is focussed in this article. In a bioreactor, the substrate concentration field and the bioreaction kinetics are strongly coupled. The latter are determined by the intensity and magnitude of concentration fluctuations encountered along the cell trajectory. Modeling these interactions between hydrodynamics and biology in heterogeneous bioreactors is a major challenge. This model is based on a previous work regarding the dynamic response of bioreactors. It is shown that a simplified population balance equation considering only growth and adaptation is sufficient to reproduce the population growth rate dynamics in batch and continuous cultures. Finally, a validation of the model implementation in a computational fluid dynamics software is proposed. The model developed in the homogeneous case now allows the numerical scale-up of a bioreactor, for it connects the population state to the concentration changes experienced. © 2012 American Institute of Chemical Engineers *AIChE J,* 59: 369–379, 2013

Keywords: bioreactor, population balance model, kinetic model, scale-up, dynamic simulation

Introduction

Competition between mixing, gas–liquid mass transfer and biological reaction is essential to explain the functioning of biological processes, especially when the scale-up issue is addressed. Comparison of the time constants of the different key phenomena is a powerful tool for the analysis of the various situations that arise during the scale-up of a bioreactor. When this methodology is applied, it shows that mixing time increases with the reactor size while the time constant associated with the biological phase remains constant.[1] This contributes to our qualitative understanding of the formation of concentration gradients at the reactor scale, which are responsible for the decrease in bioreactor performance.[2–4] The interactions between hydrodynamics and biology are, however, more complex than a competition between mixing and reaction because of the cells' ability to adapt their behavior to the concentration fluctuations they experience. The intensity and nature of bioreactions are determined by both the concentration field and the cell trajectory within the reactor. Numerous experiments have provided evidence of this strong coupling and most of them were conducted in scale-down systems in the laboratory. Dunlop and coworkers were among the first to identify the effect of micromixing on growth rate and conversion yields in continuous culture of *Saccharomyces cerevisiae*.[5–7] Later, it was shown that the uptake capacity of the cells was affected by the magnitude, duration and frequency of the feast and famine events.[8–10] Recent techniques now allow the consequences of small scale heterogeneities in the concentration field to be traced at the cell scale.[11–13] These experimental studies confirm that some heterogeneity in the cell population is induced by the fluctuations in the cells' environment. From a modeling point of view, accounting for the effects of fluctuating concentrations on the production of heterogeneity within the microbial population is a major and current challenge. Our objective in this work is to build a model that intrinsically tracks this complexity and to implement this model in commercial computational fluid dynamics (CFD) software. A CFD code is actually the most suitable tool to address the simulation of multiphase flows, including mixing, two-phase mass transfer, and reaction. In most CFD simulations of bioreactors, the bioreaction kinetics are not affected by the occurrence of concentrations gradients and the computation of the reaction terms are related to the local concentrations. It is now proposed to extend the modeling of bioreactors so as to transfer the chemical heterogeneity into a diversity of subpopulation-level biological responses, via a dynamic population balance approach.

A population balance model (PBM) is based on the concept of segregation. The principle of segregation has already been used in the study of yeasts, the internal composition of

Correspondence concerning this article should be addressed to J. Morchain at jerome.morchain@insa-toulouse.fr.

which is known to be dependent on the cell age. In a paper that can be considered as the first in the domain, Subramanian et al.[14] described growth phenomena through the use of a mass balance population model. Most PBMs published so far refer to different stages of the cell life cycle and use a partition function that redistributes an internal compound during cell multiplication.[15–20] In that sense, heterogeneity is constitutive of the biology itself. In the approach proposed here, the PBM is used to describe a biological heterogeneity induced by the environment, namely its physical, chemical, and mechanical heterogeneity.

We were not been able to find any work in the literature that combines the aspects of PBM (for the biotic phase), biological reaction, and CFD simulation. Yet such an approach makes it possible to account for the existence of multiple physiological states and to consider a biological response specific to the physiological state. By combining these two concepts, a third issue in the field of biological system modeling can be addressed, that is, the dynamic adaptation to a fluctuating environment. In the following, we describe the development of a simplified mass balance population-based model in detail and its validation in the homogeneous case. The proposed PBM is based on a previous work where the adaptation of the mean population specific growth rate was addressed.[21] Then this model is implemented in a CFD code and used to simulate the dynamic response of the population to a concentration step in a purely convective flow configuration.

Model Framework

The concept of population balance is introduced to account for heterogeneity in the biological phase as a consequence of nutrient concentration fluctuations (substrate and oxygen gradients).

Segregation of the population

The criterion chosen to discriminate among individuals is their specific growth rate μ. This choice is convenient since the domain in the μ-space is bounded and known *a priori,* so a fixed pivot technique can be used. For any individual cell, it can be written that

$$\mu \in [0; \mu_{\max}] \tag{1}$$

Secondly, let $p(\mu)$ be the probability density function in number of individuals that exhibit a specific growth rate equal to μ and let n_T be the total number of cells in the medium. The total number of cells is the integral of the distribution $p(\mu)$

$$n_T = \int_0^{\mu\max} p(\mu)d\mu \tag{2}$$

If the interval [0; $\mu_{\max}$] is divided into NC−1 subintervals, the width of each subinterval is $\Delta\mu = \frac{\mu_{\max}}{NC-1}$ and the coordinates of the NC pivots are given by the vector x

$$x(i) = \frac{(i-1)\mu_{\max}}{NC-1} \quad i = 1, .., NC \tag{3}$$

The number of cells in the ith class is calculated as follows

$$n(\mu_i) = \int_{x(i)}^{x(i)+\Delta\mu} p(\mu)d\mu \tag{4}$$

The specific growth rate in each class is then defined as

$$\mu_i = (i-1).\frac{\mu_{\max}}{NC-1} \quad i = 1, .., NC \tag{5}$$

So the Eq. 2 can now be replaced by its discrete form

$$n_T = \sum_1^{NC} n(\mu_i) \tag{6}$$

In the following, the reference to the specific growth rate is omitted, that is, $n(\mu_i)$ is noted n_i. The total biomass is thus represented by its growth rate distribution: a vector of the number of individuals in each class

$$n_T = \{n(\mu_i)\}_{1,NC} = \{n(1), n(2), .., n(NC)\} \tag{7}$$

The population specific growth rate, μ_{pop}, which can be measured experimentally, is simply written as the mean specific growth rate, or the first-order moment of the distribution divided by the zero order moment.

$$\mu_{pop} = \frac{1}{n_T}\sum_1^{NC} \mu_i.n_i \tag{8}$$

The physiological state of the population is thus related to the distribution shape. It is noteworthy that identical specific growth rates can be obtained from two distinct distributions. The question of how concentration changes influence the shape of the distribution is addressed in the next part.

Population balance equation

A population balance equation (PBE) describes the transport in both physical and internal variable space. A general formulation was proposed by Ramkrishna[22]

$$\frac{\partial n(\xi,x,t)}{\partial t} + u_i\frac{\partial n(\xi,x,t)}{\partial x_i} - \frac{\partial}{\partial x_i}\left(\Gamma\frac{\partial n(\xi,x,t)}{\partial x_i}\right) = -\frac{\partial}{\partial \xi_j}(n(\xi,t).\zeta) + h(\xi,t) \tag{9}$$

ξ is the vector of internal coordinates that are used to discriminate among individuals, x is the vector of spatial coordinates, and t is the time. The second and third terms of the left hand side are relative to the convective and diffusive transport in physical space. These are, respectively, related to the velocity field, u, and the diffusivity Γ. Just as u stands for a velocity in the physical space, ζ represents the velocity in the internal coordinate space: the rate of change of ξ with time. h is a net production term that reflects the rate of formation or destruction of individuals with a given property vector ξ. Since convective and diffusive transport terms are handled by the hydrodynamic model (using a compartment model approach or CFD), we have to focus on the transport in the internal variable space. In other words, the model can

be developed assuming a spatially homogeneous case. This enables an examination of the sole dynamic response of the population while concentration changes can be perfectly controlled. The general PBE then reduces to

$$\frac{\partial n_i}{\partial t} = -\frac{\partial}{\partial \mu}[n_i.\zeta] + h_i \tag{10}$$

The first term in the right hand side of the Eq. 10 corresponds to transport in the μ-space or transfer between the classes. It describes the number of individuals that change their growth rate μ_i into μ_{i-1} or μ_{i+1} due to favorable or unfavorable conditions in the medium (insufficient or excessive concentration with respect to their physiological state). In this first term, ζ refers to rate of change of μ with time.

$$\zeta = \frac{\partial \mu}{\partial t} \tag{11}$$

The definition of rate of change ζ is based on previous work by Morchain and Fonade.[21] In that paper, an internal variable e is introduced and used to calculate the actual specific growth rate of the whole population. The structured model proposed in that paper postulates that the microorganisms adapt their specific growth rate according to the discrepancy between their actual specific growth rate and the optimal specific growth rate in the same medium, μ_{env}. These two specific growth rates are based on a Monod law but the former uses the internal variable e whereas the latter uses the concentrations in the liquid phase. The original formulation of the rate of adaptation was written using the internal variable e. In this article, the problem is formulated in terms of specific growth rate μ. Thus, the adaptation law proposed in the previous paper is rewritten as detailed in Appendix. It can be recalled here that the formulation is slightly different depending on the sign of the difference between μ_{env} and μ_i. If this difference is positive, there is a net transport toward upper classes and the rate of change ζ^{u} can be written

$$\zeta^{\text{u}}(\mu) = \left(\frac{1}{T^{\text{u}}} + \mu\right).\frac{(\mu_{\text{env}} - \mu)}{\mu_{\max}}\frac{2\mu}{\mu_{\text{env}} + \mu} \quad \text{if} \quad (\mu_{\text{env}} - \mu) < 0, \quad \zeta^{\text{u}}(\mu) = 0 \tag{12}$$

If the difference is negative, there is a net transport toward lower classes and we have

$$\zeta^{\text{d}}(\mu) = \left(\frac{1}{T^{\text{d}}} + \mu\right).\frac{(\mu_{\text{env}} - \mu)(\mu_{\max} - \mu)}{\mu_{\max}(\mu_{\max} - \mu_{\text{env}})} \quad \text{if} \quad (\mu_{\text{env}} - \mu) > 0, \quad \zeta^{\text{d}}(\mu) = 0 \tag{13}$$

T^{u} and T^{d} are characteristic time constants that control the dynamics of the cell adaptation. An estimate of these time constants was proposed in a previous work[21]: $T^{\text{u}} = T^{\text{d}} = 1/0.8\mu_{\max}$. Transport between classes occurs when the specific growth rate afforded by the medium is different from the specific growth rate of the class considered. The transfer between classes is proportional to this difference: positive if the medium allows an increase of the growth rate, negative otherwise. Note that, for a given class, these two situations are mutually exclusive.

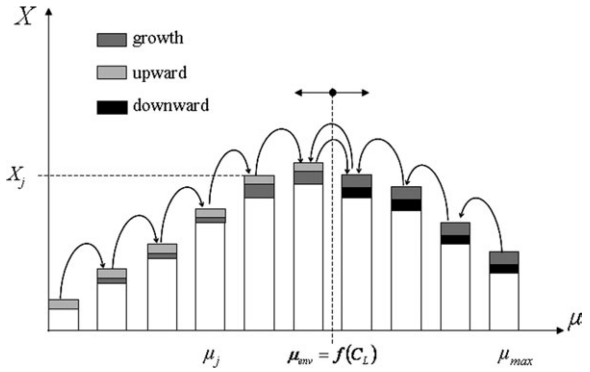

Figure 1. Schematic representation of the changes in the population growth rate distribution.

Dark gray boxes: production of new cells in the *j*th class due to growth. Light gray boxes: amount of cells in the *j*th class that will move to a class of higher index ($\mu_j < \mu_{\text{env}}$). Black boxes: amount of cells in the *j*th class that will move to a class of lower index ($\mu_j > \mu_{\text{env}}$).

In the Eq. 10, the second term on the right hand side, h_i, refers to the net flux of new organisms in the volume considered. In the field of crystallization, this last term stands for the nucleation process. In our case, it represents the birth of microorganisms in the ith class due to cell multiplication. A schematic view of transport in the μ-space and growth is presented in Figure 1. As proposed by Morchain and Fonade,[21] it is assumed that the ability to grow at a given rate is preserved through the growth process, so

$$\frac{\rho_{\text{c}} v_{\text{c}}}{V} h_i = \mu_i.X_i \quad \text{with} \quad X_i = \frac{n_i \rho_{\text{c}} v_{\text{c}}}{V} \tag{14}$$

In this equation, X_i is the biomass concentration in the ith class, expressed, for example, in $g_X\ L^{-1}$, V is the control volume, ρ_{c} and v_{c} are the cell density and cell volume respectively, which are assumed to be constants over the entire population. Under this assumption, the PBE given by the Eq. 10 can be written in terms of biomass concentration

$$\frac{\partial X_i}{\partial t} = -\frac{\partial}{\partial \mu}(X_i.\zeta) + \mu_i X_i \tag{15}$$

As already discussed by Morchain and Fonade,[21] the growth rate μ_i used in the second term of the Eq. 15 is, in practice, replaced by the actual specific growth rate, μ_i^a, defined as the minimum of μ_i and μ_{env} since cells whose growth rate μ_i is greater than μ_{env} cannot grow at their specific growth rate because they are limited by the availability of the substrate and can only achieve μ_{env}. In contrast, cells whose specific growth rate is smaller than μ_{env} are able to grow at their own specific growth rate μ_i. This leads to the definition of the actual growth rate of the population

$$\mu_{\text{pop}}^a = \frac{1}{X_{\text{T}}}\sum_1^{\text{NC}} \min(\mu_i, \mu_{\text{env}}).X_i = \frac{1}{X_{\text{T}}}\sum_1^{\text{NC}} \mu_i^a.X_i \tag{16}$$

The last step of the PBE development is to discretize the first term on the left hand side of the Eq. 15, which is done

Table 1. Model Constants used for the Chemostat Test Cases

Variable	Name	Unit	Value
Saturation constant	Ks	g L^{-1}	0.05
Saturation constant	K_{O2}	mg L^{-1}	0.1
Maximum specific growth rate	μ_{max}	h^{-1}	0.6
Yield on substrate	Y_{sX}	g_X g_S^{-1}	0.45
Yield on oxygen	Y_{so}	g_{O2} g_S^{-1}	1
Adaptation time constant	$1/T^u$, $1/T^d$	h^{-1}	0.48

using a first-order upwind scheme. By considering the two possible directions for the transport in the μ-space (upward or downward), a general expression is obtained

$$-\frac{\partial}{\partial\mu}(X_i\zeta) \cong \frac{\zeta^u(\mu_{i-1})X_{i-1} - \zeta^u(\mu_i)X_i}{\Delta\mu} + \frac{\zeta^d(\mu_i)X_i - \zeta^d(\mu_{i+1})X_{i+1}}{\Delta\mu} \quad (17)$$

Some points require particular attention:

- Adaptation is essentially a continuous process. The individuals belonging to a given class are not redistributed over the other classes as occurs when discontinuous processes such as breakage and coalescence are considered. In consequence, there is no integral term to compute in the PBE.
- At steady state, the distribution is reduced to two adjacent classes of indices i and $i + 1$ such that $\mu_i < \mu_{env}$ and $\mu_{i+1} > \mu_{env}$. The concentrations in all other classes are zero. In that case, it is straightforward to establish that

$$-\frac{\partial}{\partial\mu}(X_i\zeta) \cong \frac{-\zeta^u(\mu_i)X_i}{\Delta\mu} - \frac{\zeta^d(\mu_{i+1})X_{i+1}}{\Delta\mu} \quad (18)$$

and

$$-\frac{\partial}{\partial\mu}(X_{i+1}\zeta) \cong \frac{\zeta^u(\mu_i)X_i}{\Delta\mu} + \frac{\zeta^d(\mu_{i+1})X_{i+1}}{\Delta\mu} \quad (19)$$

In other words, at steady state, the net flux between these two classes is null, which shows that the general formulation presented is conservative. In fact, this is also true at any time under transient conditions: the transport in the μ-space results in no change in the total amount of biomass.

Biological reaction modeling

As a first step in the overall model development, a kinetic model is preferred for the sake of simplicity. The same unstructured model is used for each class. The present model corresponds to a population of strictly aerobic bacteria. The overall substrate and oxygen consumptions due to biological reactions are simply the sum of all consumptions over the classes.

$$r_S = -\frac{1}{Y_{SX}} \cdot \sum_i \mu_i^a X_i \quad (20)$$

$$r_{O_2} = -\frac{1}{Y_{SX}}\frac{1}{Y_{SO}} \cdot \sum_i \mu_i^a X_i \quad (21)$$

The specific growth rate allowed in a given environment is assumed to follow the Monod model with two substrates: glucose and oxygen.

$$\mu_{env} = \mu_{max}\frac{S}{K_S + S} \cdot \frac{O_2}{K_{O_2} + O_2} \quad (22)$$

Results

The set of Eqs. 12, 13, 15, 16, 20–22 is solved using Matlab. Since this PBM proposed here is an extension of the structured model presented in our previous work,[21] this previous model will serve as a reference for the analysis of the performance of the PBM. The model constants (physical and biological) are reported in Table 1. The reference strain chosen is *Escherichia coli*. The saturation constants, the conversion yield, and the maximum growth rate are taken from Xu et al.[23]

Sensitivity to the number of classes

Some numerical errors, dependent on the number of classes, NC, are introduced when discretizing Eq. 15. The first step of the validation is to determine an optimal number of classes allowing accurate prediction and limited computational requirements. This is done by studying the establishment of the steady-state in a 2-L chemostat. Initial conditions correspond to a population adapted to an environment containing a large amount of substrate and oxygen: all individuals are able to grow at their maximum specific growth rate and thus belong to the class of index NC, such that $\mu(NC) = \mu_{max}$. The initial substrate concentration in the reactor is set to S_0 =3 g L^{-1} (>> K_S). The feed flow rate is set to 0.25 mL s^{-1}, which corresponds to a dilution rate of 0.45 h^{-1}. The concentration of the feed is constant and equal to 2 g L^{-1}. Simulations were run with 10, 20, and 100 classes. The results are presented in Figure 2.

The first observation is that the number of classes indeed has a minimal influence on the results, especially for NC > 20. This is due to the fact that there is no integral term to compute in our model since coalescence/aggregation or breakage are not considered in the PB equation solved. In the general case, the calculations devoted to birth and death terms are the most time consuming and accurate results require a large number of classes, since accuracy relies upon a current flow number (CFL, in the μ-space) smaller than 1. According to the definition of T^u and T^d in the Eqs. 12 and 13, the maximum velocity in the μ-space is 1.8 μ_{max}, which allows the maximal time step to be determined.

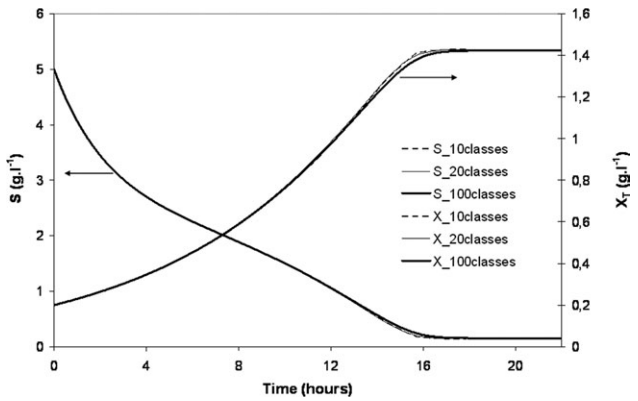

Figure 2. Transition toward the steady-state in a chemostat culture.

Influence of the number of classes for an initially adapted biomass.

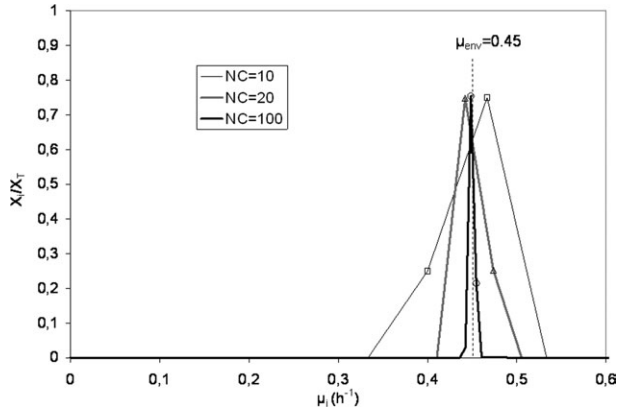

Figure 3. Final distribution at steady-state in a chemostat culture.

$$\mathrm{CFL} = \frac{\zeta_{\max}\Delta t}{\Delta\mu} \leq 1 \quad \Rightarrow \Delta t_{\max} \leq \frac{1}{1.8\,\mathrm{NC}} \tag{23}$$

All simulations were run imposing this constraint on the maximal time step length in the code solver. This explains why results are so similar.

The second observation is that the final steady-state is, as was to be expected, independent of the number of classes. When a steady-state is imposed in the environment, the whole population of cells is grouped in the two classes surrounding μ_{env}. This can be seen in Figure 3, which presents the three normalized distributions once the steady-state has been reached. The amount of cells in each of these two classes is such that $\mu_{\mathrm{pop}} = \mu_{\mathrm{env}} = D$, where D is the dilution rate. These quantities, X_i and X_{i+1}, can be calculated as the solution of the following set of equations describing global mass balances at steady sate in a perfectly mixed chemostat. The dilution rate D is equal to μ_{env} as defined in the Eq. 22

$$\begin{aligned} &D(S_0 - S) - \frac{1}{Y_{SX}}\left(\mu_i X_i + \mu_{i+1}X_{i+1}\right) = 0 \\ &-DO_2 + K_L a\left(O_2^* - O_2\right) - \frac{1}{Y_{OX}}\left(\mu_i X_i + \mu_{i+1}X_{i+1}\right) = 0 \\ &-D(X_i + X_{i+1}) + \left(\mu_i X_i + \mu_{i+1}X_{i+1}\right) = 0 \end{aligned} \tag{24}$$

The numerical solutions (X_i/X_{T} and X_{i+1}/X_{T}) obtained via a temporal integration of the PBE or via the resolution of Eq. 24 are compared in Figure 4. The data reported were obtained under various operating conditions: $D = 0.45\ \mathrm{h}^{-1}$ with 10 or 100 classes and $D = 0.36\ \mathrm{h}^{-1}$ with 20 classes. This figure shows that the stationary solutions of the PBE coincide with the solutions of the mass balances. This validates the PBM in that the population specific growth rate converges toward the correct values at steady state (D) whatever the number of classes. Now, the dynamic behavior of the PBM will be studied through the simulation of batch cultures.

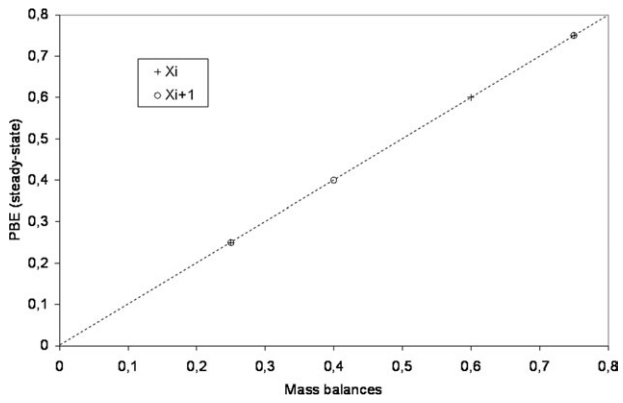

Figure 4. Comparison of the mass fraction of cells in the two classes X_i and X_{i+1} surrounding μ_{env} calculated via a mass balance or the PBM.

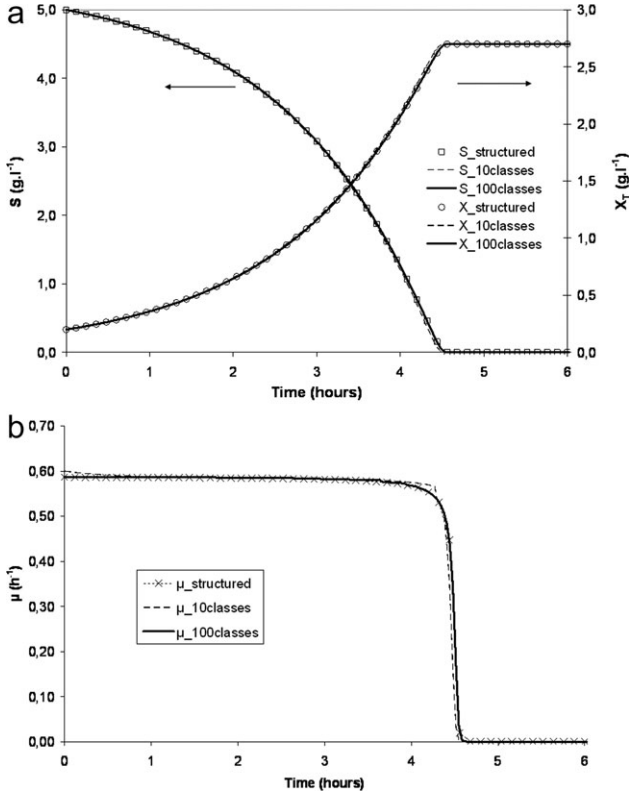

Figure 5. a. Batch culture test case #1, substrate and total biomass concentration profiles.

Comparison of the structured (open symbols) and PBM (continuous or dashed line). b. Batch culture test case #1, profiles of the actual specific growth rate obtained with the structured model (×) and the PBM with 10 classes (dashed line) and 100 classes (continuous line).

Batch test cases

The main feature of the population model is that the biomass is not necessarily adapted to its local environment. Thus, the course of a batch culture depends on the initial state of the population. Two numerical experiments were carried out to check this sensitivity to the initial conditions as well as the PBM dynamics:

- Case #1, batch culture with an initially adapted biomass (adapted to a rich environment: $S \gg K_S$). The initial specific growth rate of the population equals the environmental growth rate.
- Case #2, batch culture with a noninitially adapted biomass (adapted to a poor environment: $S = 0.25\ K_S$). The initial concentrations in the environment are the same as in case #1. The specific growth rate of all individuals is only a fifth of that possible in the environment.

The results for both experiments are presented in Figure 5 in terms of glucose and total biomass concentration (a) and

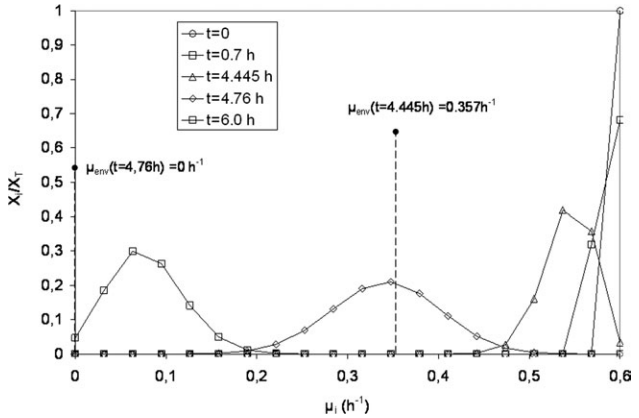

Figure 6. Normalized distribution of the population specific growth rate (mass fraction of cells able to grow at μ_i) during the batch culture for test case #1.

population specific growth rate (b). They are compared to the results obtained with the structured model under the same conditions. The first observation is that the PBM correctly reproduces the behavior of the previously published structured model.

The second observation is that the actual growth rate of the population strictly follows the growth rate imposed by the environment (Figure 5b). This is due to the limitation of μ_i to μ_{env} if $\mu_i > \mu_{\text{env}}$ already discussed after the Eq. 15. Here again, the number of classes has a minimal influence on the dynamics of the model. The changes in μ are smoother, without steep variations, when the number of classes is increased.

The normalized distribution of the population at different instants is presented in Figure 6. In this figure, the value of the environmental growth rate at some particular moments is also indicated by a vertical dashed line. In test case #1, the initial substrate concentration is high; the population is adapted to that environment so all cells belong to the highest class. As the culture proceeds, the glucose concentration diminishes and so does the environmental growth rate. Then, the point is reached where $\mu_{\text{env}} < \mu(\text{NC})$, which creates a movement in the μ_space from the class of index NC toward that of index NC$-$1. This phenomenon can be observed in particular at $t = 0.7$ h. At $t = 4.445$ h, the glucose is almost exhausted and the environmental growth rate has fallen to 0.375 h^{-1}. Yet, the population specific growth rate associated with the distribution at that time is clearly above that value, around 0.5 h^{-1}. From that point onward, the environmental growth rate falls rapidly to zero, as does the actual population growth rate, but the population specific growth rate decreases only progressively as the distribution shifts to the left. The population specific growth rate can, therefore, be considered as the specific growth rate that the population would exhibit after a sudden pulse of glucose resulting in a glucose concentration $S >> K_S$, that is, it represents the *potential* specific growth rate of the population. Such an addition at $t = 4.76$ h, (20 min after the glucose exhaustion) would lead to a population growth rate of around 0.35 h^{-1}, while the same addition at $t = 6$ h would result in a population growth rate of around 0.1 h^{-1}. This Figure 6 thus illustrates one fundamental feature of the model that introduces a decoupling between the potential growth rate of the population and the growth rate allowed by the environment.

Test case #2 deals with the sensitivity of the model to the initial conditions and presents some aspects of the model dynamics. The population is not adapted to the environment at $t = 0$ and the population growth rate is set to 0.133 h^{-1} by putting all cells a single class corresponding to that value. The results obtained with 10 classes are compared to the results given by the structured model in Figure 7a, b. Figure 7a shows that the dynamics of the PBM is very similar to that of the structured model, which confirms that the approximations made in Appendix to establish the expression for $\zeta(\mu)$ are acceptable. Because of the lower initial growth rate, the glucose and total biomass curves are pushed back. The comparison with the results of the previous case #1 (dashed line) shows that even if the same environment is imposed to both populations at $t = 0$, the growth dynamics is dependent on the previous conditions experienced by each population. These results can be regarded as the response of two populations previously adapted to high or low substrate concentrations (coming from different locations in a reactor) and exposed at $t = 0$ to the same environment. The Figure 7b shows the profiles of the actual population growth rate, the environmental growth rate as computed in the PBM and the growth rate computed with the structured model. The latter is the analog of the population actual specific growth rate. The environmental growth rate being higher than the population growth rate, a shift of the distribution toward higher

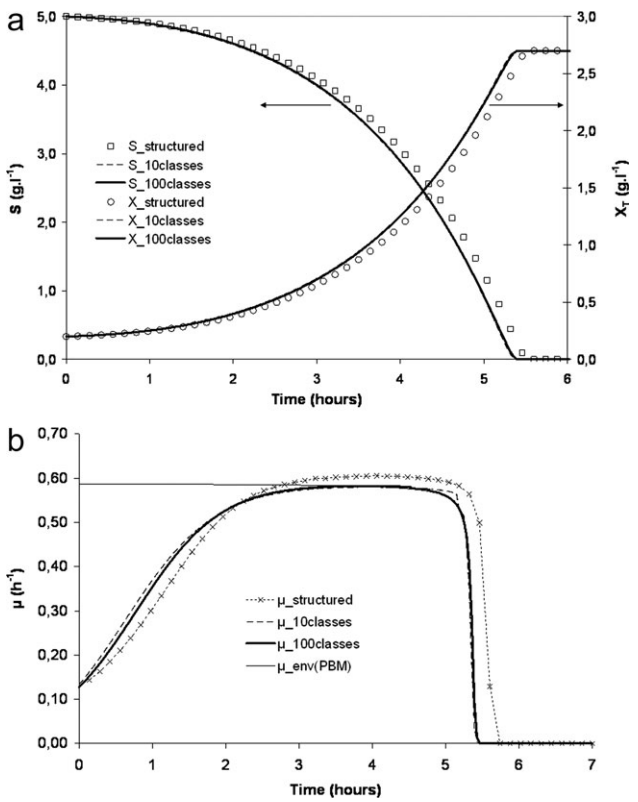

Figure 7. a. Batch culture test case #2, substrate and total biomass concentration profiles.

Comparison of the structured (open symbols) and PBM (continuous line). Results from test case #1 are recalled (dashed line). b. Batch culture test case #2, specific growth rate profiles obtained with the structured model (×) and the PBM with 10 classes (dashed line) and 100 classes (continuous thick line). Continuous line: PBM environmental growth rate.

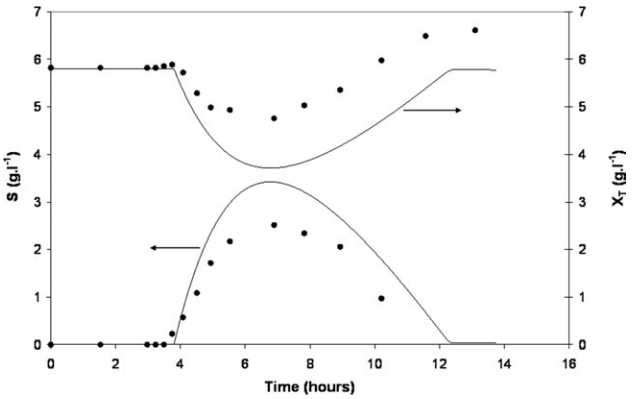

Figure 8. Transient response of a continuous culture of *Candida tropicalis* to a sudden shift in the dilution rate from $D = 0.1$ to 0.4 h^{-1}.

Continuous line: PBM.

classes takes place and the population specific growth rate progressively increases. The dynamics is almost independent of the number of classes and is very similar to that obtained with the structured model. The population specific growth rate finally becomes limited by μ_{env} shortly after 3 h of batch culture. The slight differences observable in Figure 7b between the profiles of μ_*structured* and μ_10*classes* (or μ_100*classes*) are due to the fact that the concentration profiles in Figure 7a are not exactly the same. This is a consequence of the approximations made when defining the rate of change $\zeta(\mu)$.

Comparison with experimental data

The PBM kinetic model is now compared to an experimental data set from the work of Kätterer et al.[24] Kätterer and coworkers have reported the data from continuous cultures of *Candida tropicalis* performed in a 3-L reactor, equipped with a two-stage stirrer rotating at 1000 rpm, under conditions of limiting glucose (concentration below 10 mg L^{-1}) and sufficient oxygen ($pO_2 > 50\%$). After a batch growth phase, cells were transferred into a chemostat and cultivated at a dilution rate of 0.1 h^{-1} until a steady-state was reached (e.g., during more than 7 volume changes). A step increase in the dilution rate from 0.1 to 0.42 h^{-1} was applied to the reactor. The biological characteristics of the strain are given in the cited paper ($\mu_{max} = 0.52$ h^{-1}) and the saturation constant and yield were deduced from the steady-state ($K_S = 10$ mg L^{-1}, $Y_{SX} = 0.61$). The same biological parameters are used for the simulation and the population is considered adapted to the environment prior to the step increase of the dilution rate. The results are presented in Figure 8, which compares the experimental profiles of biomass and substrate to those predicted by the simulation. The dynamics of the transition between two steady-states is well described but the biomass concentration level is not, because a constant yield Y_{SX} is used. It was shown in a previous paper that the introduction of a Pirt's law expression, $Y_{SX} = f(\mu)$, allowed much better prediction of the concentration levels without affecting the transition dynamics. Considering a variable yield could constitute a future improvement for the biological reaction part of the model but it is not considered as essential at the moment.

Coupling with CFD simulation

The PBM was implemented in the CFD code Fluent via a user defined function. The number of classes was set to NC = 10 to limit the computational requirements. The formal analogy between the set of equations describing the spatial evolution of the concentrations in an ideal plug flow reactor (dispersion neglected) and the temporal evolutions in a perfectly mixed reactor operated in batch mode was used to design a test case. The equation for the batch case is Eq. 10. Considering the change of variable, $u = x/t$, this equation leads to Eq. 25 that stands for the steady-state simulation of the ideal plug flow.

$$u_i \frac{\partial n(\xi, x, t)}{\partial x_i} = -\frac{\partial}{\partial \xi_j}(n(\xi, t).\zeta) + h(\xi, t) \tag{25}$$

The plug flow reactor was simulated with Fluent software, the batch reactor is simulated with a personal code developed in Matlab. In both codes, population balance dynamics, biological reaction, and oxygen mass transfer were considered. The same set of equations with identical parameter values, given in Table 2, was solved. The ideal gas–liquid plug flow was first simulated in Fluent with a Euler-Euler approach. The liquid phase velocity, u, was chosen such that the residence time in the plug flow reactor of length L equaled the duration of the batch simulation $t = L/u$ (Figure 9). Once the velocity field for each phase and the gas volume fraction had been computed, these variables were frozen and the scalar equations for the biomass, substrate and oxygen in both phases were solved. A constant bubble size and mass-transfer coefficient K_L were imposed, leading to the same K_La for both simulations. Its value was chosen to ensure high oxygen concentrations in the medium. The initial conditions of the batch simulation correspond to the inlet conditions for the CFD simulations. A uniform distribution of the total biomass among the 10 classes was prescribed. The ratio between initial substrate and initial biomass was such that complete exhaustion would take place during the simulation. The results obtained with the CFD simulation of the ideal plug flow were compared to those obtained with the simulation of a batch culture in a perfectly mixed reactor using a Matlab code. The total biomass and substrate profiles are reported in Figure 10. The biomass profiles for four of the 10 classes are presented in Figure 11. The abscissa in Figures 10 and 11 is expressed in time unit but it actually corresponds to the distance from the inlet of the plug flow reactor, which has been converted into a residence time. Perfect agreement can be observed, which indicates that the different equations have been correctly implemented and solved within each code. The total biomass and substrate profiles are typical of a batch culture. The global mass balances are satisfied since 0.75 g of additional biomass is produced while

Table 2. Model Constants used for the CFD Simulation

Variable	Unit	Value
Ks	g L^{-1}	0.05
μ_{max}	h^{-1}	1
Duration	h	1.67
S inlet	g L^{-1}	1.5
X_T inlet	g L^{-1}	1
Y_{SX}	g_X g_S^{-1}	0.5
$1/T^u$	h^{-1}	0.9
$1/T^d$	h^{-1}	0.9

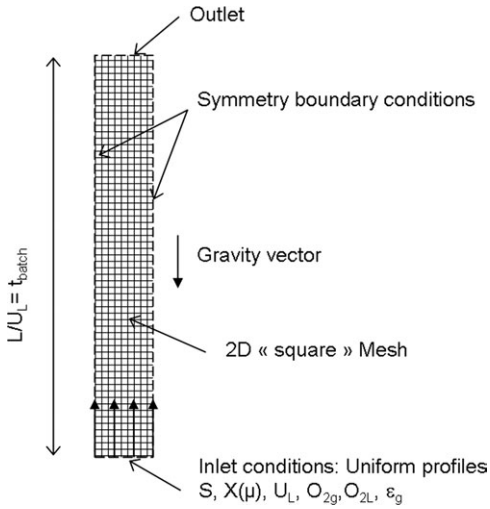

Figure 9. Set-up of the CFD model for the simulation of the ideal plug flow.

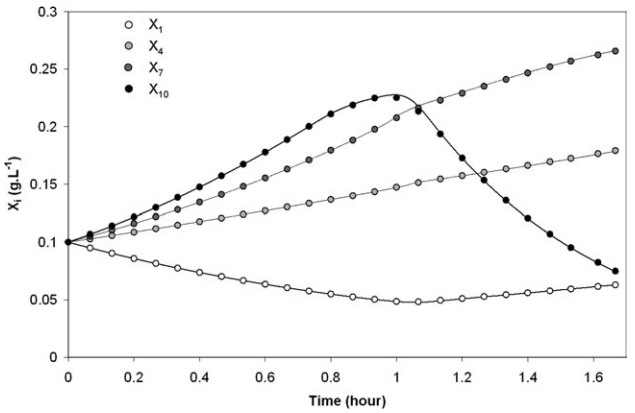

Figure 11. Implementation of the PBM in the CFD simulation: comparison of the biomass concentrations in classes #1, 4, 7, and 10.

Symbols: plug flow model (CFD), continuous lines: batch culture (Matlab simulations).

1.5 g of substrate is consumed. Moreover, the concentration profiles of the different classes help our understanding of the complex relationship among the concentration of the substrate, the actual growth rate of the population, and the changes in the shape of the distribution. The initial substrate concentration is high (far above K_S) so $\mu_{env} = \mu_{max}$. Since the initial distribution is uniform, the initial population growth rate is only half the maximum specific growth rate, i.e. $\mu_{pop}(0) \cong 0.3\ h^{-1}$. The environment is rich in substrate; the population specific growth rate can increase. This results in a movement toward the right in the μ-space. Additionally, growth increases the amount of cells within each class. Before substrate exhaustion (around 3800s), X_1 decreases continuously because the mass transfer term toward class #2 dominates growth in class #1. X_{10} increases because of mass transfer from class # 9 and growth. The other two classes are subject to growth and mass transfer which, in these cases, contains two terms (from the lower class and toward the upper class). From $t = 3000$ s, the net rate of accumulation of class #10 becomes slower. Just before substrate exhaustion, this rate becomes negative and the amount of cells in class #10 starts decreasing because the environmental growth rate is falling rapidly to zero. After glucose exhaustion, a movement from the right to the left in the μ-space takes place. The amount of cells in class #10 now decreases sharply and this fuels the classes of lower indices. It should be noted that, despite the increase of X_1, X_4, and X_7, the population specific growth rate indeed decreases; while the actual population growth rate is null as imposed by the environment. Figure 12 shows how the normalized specific growth rate distribution responds dynamically to the changes in the environment. This figure illustrates once again that heterogeneity in the biological phase persists in a homogeneous environment. Owing to the modeling approach adopted here, the shape of the normalized distribution results from both the local composition of the environment and the history of the population.

Discussion

Chung and Stephanopoulos[25] have proved the existence of heterogeneities in a population of *E. coli* bacteria grown in a common environment. The presence of multiple physiological states among individuals in the same culture is consistent with the fact that biological systems can be described by a large number of coupled mass balance equations for which multiple solutions are known to exist. Multiple solutions are frequently encountered in systems of strongly coupled

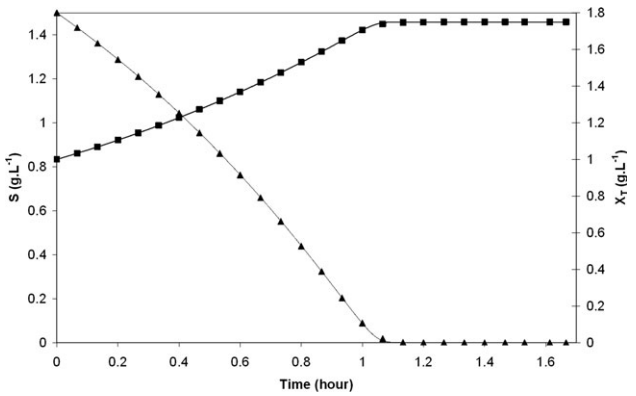

Figure 10. Implementation of the PBM in the CFD simulation: comparison of the total biomass and substrate profiles.

Symbols: plug flow model (CFD), continuous lines: batch culture (Matlab simulations).

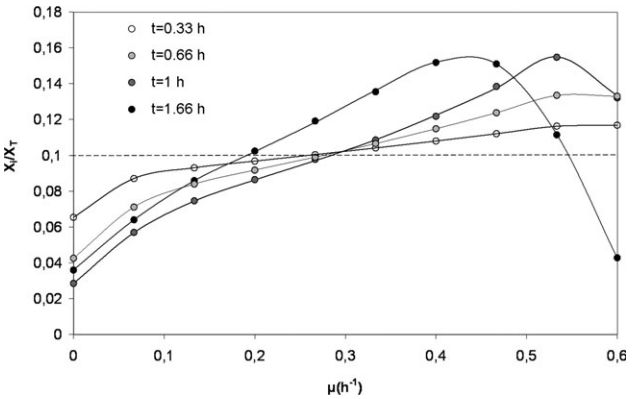

Figure 12. Normalized distributions at different residence times (eq. locations) in the plug flow reactor.

Symbols: plug flow model CFD, continuous line: batch culture (Matlab simulations).

nonlinear equations. Chung and Stephanopoulos explain that nonlinearity arises from regulatory mechanisms such as feedback existing in microorganisms. Thus, the simultaneous occurrence of multiple physiological states may be considered as a fundamental characteristic of a biological population.[25] According to these authors, the physiological homogeneity frequently assumed in both experimental and theoretical analysis of cell behavior lacks theoretical justification.

As far as this biologically induced heterogeneity (constitutive heterogeneity) is concerned, it is nowadays taken into account via PBM that distinguish between the different phases during the cell life cycle. The heterogeneity within the population arises from a partition function that redistributes an internal compound unevenly among the newborn cells. As already mentioned, this requires the computation of an integral term in the PBE. The noteworthy point here is that the associated time scale of these models is much shorter than the time scale for growth.

In this work, we are interested in externally induced heterogeneity, that is, physiological heterogeneity as a consequence of external fluctuations (concentration, pH, mechanical stress, etc.). Of course, the two mechanisms producing heterogeneity within the biological population are not mutually exclusive. In many industrial situations, one may fear a combined effect of these two contributions and this makes the analysis of the relationship between operating conditions and biological response even more tedious. To perform a validation in a clearly identifiable situation, we focused on the development of the PBM in the so-called homogenous case. If the spatial derivatives are discarded in Eq. 9, it implies that the bioreactor is perfectly mixed. The fact that the reactor is perfectly mixed means that all cells will be exposed to the same concentration, but this concentration can vary in time. In this work, all cells are simultaneously exposed to a single concentration step. This allows the examination of the dynamic response of the population solely. The way concentrations changes are imposed can be used to reproduce the fate of cells in a large scale bioreactor. The magnitude of the concentration change itself mimics the fact that a volume of fluid containing cells is passing close to the feed point in a macroscopically heterogeneous bioreactor. The frequency can be related to the mean circulation time. Therefore, the model presented here can be used, as it is, to perform scale-down experiments: the study the effect of repeated pulse additions of substrate in a batch reactor, a method which is commonly used to mimic the effect of concentration gradients occurring in large scale reactors as explained by Neubauer and Junne[26] in a recent review.

In the continuity of a previous work, our choice was to build a model that accounted for the adaptation of the population growth rate. It has been shown that the time scale associated with this model is of the same order as the time scale for growth. In our model, the population is discriminated according to the specific growth rate and the adaptation dynamics is controlled by a time constant Ta # $1/\mu_{max}$. So, it naturally makes sense to combine this population model with a hydrodynamic model consisting of a number of interconnected perfectly mixed reactors, provided each reactor has a residence time of about $1/\mu_{max}$. There are indeed many various time scales associated to the biology of the cell. Another biological phenomenon can be considered leading to a different time constant. In case this time constant is comparable to the mixing time of the bioreactor then it is thought that the combination of PBM and CFD represents the most promising and rigorous approach.

In our model, the biologically induced heterogeneity is filtered: growth in a given class does not produce heterogeneity within this class. In consequence, there is no partition function and no integral term to compute in the proposed PBM, which can, therefore, be regarded as a subpopulation model. Because there is no integral term to compute, the accuracy of the model is independent of the number of classes provided that a condition on the CFL in the μ-space is satisfied. One characteristic of the biological model also contributes to this particular feature of the PBM: the glucose uptake rate is directly linked to the specific growth rate via Y_{SX}. There is much experimental evidence indicating that the instantaneous substrate uptake rate and the specific growth rate are indeed decoupled.[8,10,27–30] The consequence on the calculation of the actual uptake rate has been thoroughly discussed in a previous work,[21] where it was concluded that:

1. The actual uptake rate should be based on the concentration in the liquid phase.
2. It is independent of the specific growth rate.

Adapting these conclusions to the present model means that, in classes where μ_i is lower than μ_{env}, the uptake rate exceeds the utilization rate for (balanced) growth. The fate of the extra amount of substrate is a matter of intracellular biology but one crucial point is the correct estimation of the accumulation rate $\phi_{S,acc}$ in $g_S\ s^{-1}$. For each class, this can be easily expressed from the difference between the actual uptake rate and the utilization rate. At the population scale, this leads to the following equation

$$\varphi_{S,acc} = \int_0^{\mu_{env}} \frac{(\mu_{env} - \mu_i)}{Y_{SX}} . X_i . d\mu \tag{26}$$

Since there is now an integral term in the PBM, the number of classes is essential because it affects the shape of the distribution, that is, the amount of cells in each class, and thus the accuracy of the integral presented in Eq. 26.

In the present form, our choice of a limited number of classes reduces the computational cost of the simulation but does not affect the generic character of the observations made:

1. The growth rate distribution reflects the history of the concentration field encountered and it evolves with the local conditions.
2. The PBM is a convenient tool to address the issue of interactions between physical heterogeneity and physiological heterogeneity.
3. The PBM can be incorporated in the framework of a CFD code.

This discussion, therefore, points out that the representation of the population and the model for biological reactions are far from being independent.

Conclusion

A population model accounting for the adaptation of a microbial population to a changing environment was developed and validated against an existing model as well as experimental data. In a previous paper, the concept of inertia in the dynamic response of the population was introduced leading to a structured model. However, the fate of each individual was not considered and the whole population was described by a single internal variable. The population balance approach enlarges the capabilities of that model for it considers the distribution of the internal variable within the population. In this article, the method of class is used to solve the PBE. The internal variable chosen is the specific growth rate that is

assumed to be different between individuals and from that defined by the concentrations of substrates in the liquid phase. The model is used to predict the changes in the population growth rate as a response to some changes in the environment. A kinetic model is used to define the reaction rates due to the biological activity. The influence of the number of classes on the results was shown to be minimal. In this context, it was shown that the proposed PBM correctly represents the specific growth rate dynamics. Therefore, this type of model correctly handles the issues regarding the mixing of distinct populations and the consequences of external fluctuations on the actual specific growth rate of the microbial population. The PBM model proposed was also implemented in the CFD code FLUENT and successfully validated. This work can now serve for a rational approach of scale-up issues in bioreactors by taking into account the two way coupling between velocity/concentration fields and population dynamics. In the present work, a single parameter was chosen to segregate the population. However, it is obvious that the description of the cell dynamics should refer to more than one parameter. Thus, future works should focus on the formulation of a multidimensional PBM for bioreactions along with suitable solving methods.

Notation

h_i = net flux of new cells in the ith class, g L^{-1} s^{-1}
$K_L a$ = mass-transfer coefficient, s^{-1}
K_S = affinity constant for the substrate, g L^{-1}
K_{O2} = affinity constant for oxygen, g L^{-1}
NC = number of classes
n_i = number of cells in the ith class
n_T = total number of cells
$[O_{2gas}]$ = local oxygen concentration in the gas, g L^{-1}
$[O_{2liq}]$ = local oxygen concentration in the liquid, g L^{-1}
O_{2X}^{pop} = respiratory capacity of a cell, g g_X^{-1}
O_2^{pop} = respiratory capacity of the population, g L^{-1}
$[O_2]^*$ = local saturation concentration, g L^{-1}
r_S = reaction rate for substrate, g_S^{-1} s^{-1}
r_{O2} = reaction rate for oxygen, g_{O2}^{-1} s^{-1}
r_{Xi} = reaction rate for the ith class of biomass, g_X^{-1} s^{-1}
S = local substrate concentration, g L^{-1}
v_c = volume of one cell, m^3
X_i = concentration of cells in the ith class, g L^{-1}
X_T = total concentration of cells, g L^{-1}
Y_{OX} = yield coefficient of oxygen per unit of biomass, g_X g_{O2}^{-1}
Y_{SX} = yield coefficient of substrate per unit of biomass, g_X g_S^{-1}

Superscripts

d = downward, transfer toward a class of lower index
u = upward, transfer toward a class of higher index

Subscript

i = class index

Greek letters

ζ = rate of change of specific growth rate, s^{-2}
μ = specific growth rate, s^{-1}
μ_{env} = specific growth rate that the biomass can reach, s^{-1}
μ_{max} = maximum specific growth rate, s^{-1}
μ_{pop} = population specific growth rate, s^{-1}
Φ = net rate of substrate accumulation g_S s^{-1}

Literature Cited

1. Amanullah A, McFarlane CM, Emery AN, Nienow AW. Scale-down model to simulate spatial pH variations in large-scale bioreactors. *Biotechnol Bioeng*. 2001;73:390–399.
2. George S, Larsson G, Olsson K, Enfors S-O. Comparison of the baker's yeast process performance in laboratoty and production scale. *Bioprocess Eng*. 1998;18:135–142.
3. Larsson G, Törnkvist M, Wernersson ES, Trägårdh C, Noorman H, Enfors SO. Substrate gradients in bioreactors: origin and consequences. *Bioprocess Biosystems Eng*. 1996;14:281–289.
4. Lara AR, Galindo E, Palomares LA, Ramírez OT. Living with heterogeneous bioreactors: understanding the effect of environmental gradients in cells. *Mol Biotechnol*. 2006;34:355–381.
5. Dunlop EH, Ye SJ. Micromixing in fermentors: metabolic changes in *Saccharomyces cerevisiae* and their relationship to fluid turbulence. *Biotechnol Bioeng*. 1990;36:854–864.
6. Fowler JD, Dunlop EH. Effect of reactant heterogeneity and mixing on catabolite repression in cultures of Saccharomyces cervisiae. *Biotechnol Bioeng*. 1989;33:1039–1046.
7. Wenger KS, Dunlop EH. Coupling of micromixing, macromixing and the glucose effect in continuous culture of Saccharomyces cerevisiae. *Ind Mixing Technol—AIChE Symp Ser*. 1994;90:166–174.
8. Lin YH, Neubauer P. Influence of controlled glucose oscillations on a fed-batch process of recombinant Escherichia coli. *J Biotechnol*. 2000;79:27–37.
9. Lin HY, Mathiszik B, Xu B, Enfors SO, Neubauer P. Determination of the maximum specific uptake capacities for glucose and oxygen in glucose-limited fed-batch cultivations of *Escherichia coli*. *Biotechnol Bioeng*. 2001;73:347–357.
10. Neubauer P, Häggström L, Enfors SO. Influence of substrate oscillations on acetate formation and growth yield in *Escherichia coli* glucose limited fed-batch cultivations. *Biotechnol Bioeng*. 1995;47:139–146.
11. Lara AR, Leal L, Flores N, Gosset G, Bolívar F, Ramírez OT. Transcriptional and metabolic response of recombinant *Escherichia coli* to spatial dissolved oxygen tension gradients simulated in a scale-down system. *Biotechnol Bioeng*. 2006;93:372–385.
12. Garcia JR, Cha HJ, Rao G, Marten MR, Bentley WE. Microbial nar-GFP cell sensors reveal oxygen limitations in highly agitated and aerated laboratory-scale fermentors. *Microb Cell Fact*. 2009;8:6
13. Delvigne F, Ingels S, Thonart P. Evaluation of a set of E. coli reporter strains as physiological tracer for estimating bioreactor hydrodynamic efficiency. *Process Biochem*. 2010;45:1769–1778.
14. Subramanian G, Ramkrishna D, Fredrickson A, Tsuchiya H. On the mass distribution model for microbial cell populations. *Bull Math Biol*. 1970;32:521–537.
15. Fredrickson AG. Population balance equations for cell and microbial cultures revisited. *AIChE J*. 2003;49:1050–1059.
16. Fredrickson AG, Mantzaris NV. A new set of population balance equations for microbial and cell cultures. *Chem Eng Sci*. 2002;57:2265–2278.
17. Mantzaris NV. A cell population balance model describing positive feedback loop expression dynamics. *Comput Chem Eng*. 2005;29:897–909.
18. Mantzaris NV, Daoutidis P. Cell population balance modeling and control in continuous bioreactors. *J Process Control*. 2004;14:775–784.
19. Mantzaris NV, Srienc F, Daoutidis P. Nonlinear productivity control using a multi-staged cell population balance model. *Chem Eng Sci*. 2002;57:1–14.
20. Stamatakis M. Cell population balance, ensemble and continuum modeling frameworks: conditional equivalence and hybrid approaches. *Chem Eng Sci*. 2010;65:1008–1015.
21. Morchain J, Fonade C. A structured model for the simulation of bioreactors under transient conditions. *AIChE J*. 2009;55:2973–2984.
22. Ramkrishna D. Solution of population balance equations. *Chem Eng Sci*. 1971;26:1134–1136.
23. Xu B, Jahic M, Enfors SO. Modeling of overflow metabolism in batch and fed-batch cultures of *Escherichia coli*. *Biotechnol Prog*. 1999;15:81–90.
24. Kätterer L, Allemann H, Käppeli O, Fiechter A. Transient responses of continuously growing yeast cultures to dilution rate shifts: a sensitive means to analyze biology and the performance of equipment. *Biotechnol Bioeng*. 1986;28:146–150.
25. Chung JD, Stephanopoulos G. On physiological multiplicity and population heterogeneity of biological systems. *Chem Eng Sci*. 1996;51:1509–1521.
26. Neubauer P, Junne S. Scale-down simulators for metabolic analysis of large-scale bioprocesses. *Curr Opin Biotechnol*. 2010;21:114–121.
27. Ferenci T. Growth of bacterial cultures 50 years on: towards an uncertainty principle instead of constants in bacterial growth kinetics. *Res Microbiol*. 1999;150:431–438.
28. Leegwater MPM, Neijssel OM, Tempest DW. Aspects of microbial physiology in relation to process control. *J Chem Technol Biotechnol*. 1982;32:92–99.

29. Natarajan A, Srienc F. Dynamics of glucose uptake by single *Escherichia coli* cells. *Metab Eng*. 1999;1:320–333.
30. Natarajan A, Srienc F. Glucose uptake rates of single *E. coli* cells grown in glucose-limited chemostat cultures. *J Microbiol Methods*. 2000;42:87–96.

Appendix

In a previous work, a single variable e (in $g_e\ g_X^{-1}$) was introduced to describe the dynamic behavior of a population of cells subjected to sudden changes its environment. The main equations proposed were

The conservation equation for e over a volume V flushed by the flow rate Q

$$\frac{d(X.e.V)}{dt} = Q.X.e|_{\text{in}} - Q.X.e + r_e.V + A_e.X.V \tag{A1}$$

The adaptation rate of the whole population

$$A_e = \delta q_+(e^* - e)\frac{2e}{e^* + e} + (1-\delta)q_-(e^* - e)$$
$$\delta = 1 \quad \text{if } e^* > e \text{ and } \delta = 0 \text{ otherwise} \tag{A2}$$

A kinetic constant

$$q = \frac{1}{\tau} + \mu^b \tag{A3}$$

A law of equilibrium relating the actual specific growth rate to the internal variable e

$$\mu^b = \mu_{\max}\prod_i \frac{e_i}{k_{e_i} + e_i} \tag{A4}$$

In that work, only one variable e was considered. Thus, e can be expressed as a function of μ

$$\mu = \mu_{\max}\frac{e}{k+e} \tag{A5}$$

It can be recalled here that e^* is the value of e when a steady-state is reached, that is, when the population and its environment are in an equilibrium state, which is expressed mathematically as $\mu(e^*) = \mu_{\text{env}}$

The rate of change $\zeta(\mu)$ can be written as

$$\zeta(\mu) = \frac{\partial \mu}{\partial t} = \frac{\partial \mu}{\partial e}.\frac{\partial e}{\partial t} = \frac{\mu_{\max}k}{(k+e)^2}.Ae$$

If the difference $(e^* - e)$ (or equivalently $\mu^* - \mu$) is positive, the combination of Eqs. A2 and A5 leads to the expression for the rate of change $\zeta(\mu)$

$$\zeta(\mu) = \frac{\mu_{\max}k}{(k+e)^2}\left(\frac{1}{T} + \mu\right).(e^* - e).\frac{2e}{e^* + e} \tag{A6}$$

To express this rate as a function of μ only, we can consider the following expressions

$$\frac{\mu_{\text{env}} - \mu}{\mu_{\max}} = \frac{e^*}{k + e^*} - \frac{e}{k+e} = \frac{k}{(k+e^*)(k+e)}(e^* - e) \tag{A7}$$

and

$$\frac{2e}{e^* + e} = \frac{2\mu}{\mu_{\text{env}}\frac{\mu_{\max} - \mu}{\mu_{\max} - \mu_{\text{env}}} + \mu} \approx \frac{2\mu}{\mu_{\text{env}} + \mu} \tag{A8}$$

If we observe that $(k + e^*)$ and $(k + e)$ are of the same order of magnitude, these expressions can be simplified and, also using the Eq. A6 we obtain

$$\zeta(\mu) \cong \frac{\mu_{\max}k}{(k+e)^2}\left(\frac{1}{T} + \mu\right).\frac{(\mu_{\text{env}} - \mu)}{\mu_{\max}}\frac{(k+e^*)(k+e)}{k}.\frac{2\mu}{\mu_{\text{env}} + \mu} \tag{A9}$$

This expression can be finally simplified to

$$\zeta(\mu) = \left(\frac{1}{T} + \mu\right)(\mu_{\text{env}} - \mu).\frac{2\mu}{\mu_{\text{env}} + \mu} \tag{A10}$$

Respiratory capacity dynamics

Spatial integration over an elementary volume of fluid containing a large number of microorganisms leads to the definition of a macroscopic state variable, O_2^{pop}.

$$O_2^{\text{pop}} = X_T.O_{2X}^{\text{pop}} \tag{A11}$$

The population respiratory capacity, O_2^{pop}, is transported along with the group of microorganisms it characterizes: it is treated as a dissolved species in the transport equations.

In a previous paper, a general expression for the conservation equation of a state variable was proposed and used to model the adaptation of the growth rate to changing conditions (Morchain and Fonade, 2009). The same formulation is applied here to describe the dynamics of the respiratory capacity of the population. Although its chemical identity is not specified, the biological variable O_2^{pop} is taken as an extensive variable, expressed in arbitrary units per gram of biomass, so a conservation equation for O_2^{pop} over an elementary volume is written

$$\frac{d(X.O_2^{\text{pop}}.V)}{dt} = Q.X.O_2^{\text{pop}}|_{\text{in}} - Q.X.O_2^{\text{pop}} + r_{O_{\text{pop}}^2}.V + A_{O_{\text{pop}}^2}.X.V \tag{A12}$$

Where

$$r_{O_2^{\text{pop}}} = \sum_i \mu_i X_i.O_2^{\text{pop}} \tag{A13}$$

and

$$A_{O_2^{\text{pop}}} = \delta q_+\left(O_2^* - O_2^{\text{pop}}\right)\frac{2O_2^{\text{pop}}}{O_2^* + O_2^{\text{pop}}} + (1-\delta)q_-\left(O_2^* - O_2^{\text{pop}}\right)$$
$$\delta = 1 \quad \text{if } O_2^* > O_2^{pop} \text{ and } \delta = 0 \text{ otherwise} \tag{A14}$$

Manuscript received Sept. 6, 2011, and revision received Mar. 30, 2012.